An Automatic Tool for Quantification of Nerve Fibres in Corneal Confocal Microscopy Images

Xin Chen, Jim Graham, Mohammad Dabbah, Ioannis N. Petropoulos, Mitra Tavakoli, Rayaz Malik

Abstract—*Objective*: We describeand evaluatean automated software tool for nerve fibre detection and quantification in corneal confocal microscopy (CCM) images, combining sensitive nerve fibre detection with morphological descriptors. *Method*: We have evaluated the toolfor quantification of Diabetic Sensorimotor Polyneuropathy (DSPN) using both new and previously published morphological features.The evaluation used 888 images from 176 subjects (84 controls and 92 patients with Type 1 diabetes). The patient group was further subdivided into those with (n=69) and without (n=23) DSPN. *Results*: We achieve improved nerve-fibre detection over previous results (95% sensitivity and specificityin identifying nerve-fibre pixels). Automatic quantification of nerve morphology shows a high correlation with previously reported, manually measured, features. ROC analysis of both manual and automatic measurement regimes resulted in similar resultsin distinguishing patients with DSPN from those without: AUC of about 0.78 and 72% sensitivity/specificity at the equal error rate point. *Conclusion*: Automated quantification of corneal nerves in CCM images provides a sensitive tool for identification of DSPN. Its performance is equivalent to manual quantification, while improving speed and repeatability. *Significance*: Corneal confocal microscopy is a novel in-vivo imaging modality that has the potential to be a non-invasive and objective image biomarker for peripheral neuropathy. Automatic quantification of nerve morphology is a major step forward in the early diagnosis and assessment of progression, and, in particular, for use in clinical trials to establish therapeutic benefit in diabetic and other peripheral neuropathies.

Index Terms—Diabetic Sensorimotor Polyneuropathy, Computer Aided Diagnosis, Corneal Confocal Microscopy, Image Analysis, Nerve Fibre Quantification

1 Introduction

Diabetic sensorimotor polyneuropathy (DSPN) is one of most common long term complications of diabetes. Up to 50% of diabetic patients suffer from it [1], and it is estimated that about one in six diabetic patients have chronic painful neuropathy [2]. Several methods are currently used to quantify neuropathy, including clinical scoring of symptoms, quantitative sensory testing, nerve conduction measurements and microscopic measurement of intra-epidermal nerve-fibre density in skin biopsy samples.These methods have their advantages and limitations. Thus, whilst symptoms and signs are directly relevant to the patient and are easily recorded, they aresubjective resulting in poor repeatability [3]. Neurophysiology is moreobjective; however it only assesses large fibres, which constitute a tiny proportion of all the nerve fibres present in a peripheral nerve and have also been shown to have limited reproducibility [4]. The quantification of intra-epidermal nerve fibre density in skin biopsies is objective, but is clearly invasive and requires considerable expertise in assessment. There is a need for a rapid, non-invasive assessment that is truly quantitative and assesses small nerve fibres, which are more likely to be involved in neuropathy [5, 6].

Corneal confocal microscopy (CCM) images of nerve fibres are captured from the sub-basal plexus immediately above Bowman's membrane of the cornea by an in-vivo laser confocal microscope. Fig. 1a shows an example image. One of the advantages of CCM is the entirely non-invasive and relatively rapid (about 2 minutes) acquisition of images of small nerve fibres and other corneal structures. Clinical studies [7] have shown that CCM is capable of making quantitative assessment of DSPN and has the potential to be an ideal surrogate endpoint. It has also recently been shown to have a predictive ability inidentifying diabetic patients at risk of developing DSPN [8] and has been used in several clinical intervention studies showing nerve fibre repair [9-11]. Interactive analysis has been used to derive measurements from these images, such as corneal nerve fibre length (CNFL), corneal nerve fibre density (CNFD) and corneal nerve branch density (CNBD) [12, 13] (Fig. 1). CNFL is defined as the total length of all nerve fibres visible in the CCM image per square millimetre. CNFD and CNBD are the number of

- *J. Graham is with the Centre for Imaging Siences, the University of Manchester, UK. E-mail: jim.graham@manchester.ac.uk*
- *X. Chen is now at the Division of Imaging Sciences and Biomedical Engineering, Kings College London, UK*
- *M. Dabbah is currently at Roke Manor Research Ltd. Romsey, UK*
- *I. Petropoulos, M. Tavakoli and Rayaz Malik are with Centre for Endocrinology & Diabetes, Institute of Human Development, Manchester, UK. I. Petropoulos and Rayaz Malik are also with Weill Cornell Medical College in Qatar, Division of Medicine, Doha, Qatar.*

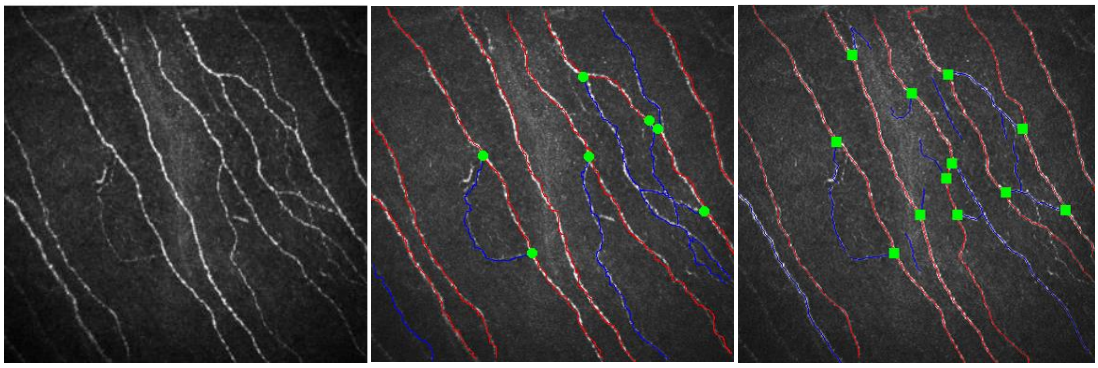

(a) (b) (c)

Fig. 1. (a) Original CCM image.(b) Manually quantified CCM image. (c) Automatically quantified CCM image. Red lines represent main nerve fibres, blue lines are branches and green spots indicate branch points on the main nerve trunks. Refer to online coloured version.

the major nerves (red lines in Fig. 1b) per square millimetre and the number of primary branchesemanating from those major nerve trunks (green dots in Fig. 1b) per square millimetre respectively. Although an association has been demonstrated between these quantitative features and the severity of DSPN [7] in cross sectional studies, the manual analysis suffers from the usual problems of being labour-intensive and subjective and therefore raises considerable difficulties, particularly when undertaking longitudinal follow-up studies [14]. Consequently the quantification results show poor reproducibility, especially in CNBD [15]. For the technology to be clinically useful, the analysis of images needs to be done automatically.

Here we describe a fully automatic nerve fibre detection and quantification system. Fig. 1a indicates that the appearance of nerve fibres in CCM images covers a wide contrast range, with some fibres appearing very faint on a noisy background, whilst other, larger, fibres show strong contrast. A number of studies have presented methods of detecting similar linear structures in different types of images e.g. the detection of blood vessels in retinal images [16], and the detection of curvilinear structure in mammograms [17]. Previous studies aimed at automatic fibre detection in CCM images include Scarpa et al. [18] who described a method for tracing nerve fibres based on automatically initialised seed points, and Holmes et al. [19] who indentified fibres based on ridge points. Sindt et al. [20] detected several types of objects visible in CCM images, including dendritic immune cells and wing cells in addition to nerve fibres. Dabbah et al. [21] presented a method of fibre detection based on a multi-scale Gabor filter with responses trained using a neural network. The best detection performance in various applications are achieved using methods based on machine learning, in which features are derived from training images.[16, 17, 21].

Following fibre detection, it is required to extract individual fibres, identify branches and quantify appropriate features for classification. A number of studies have investigated the quantification of a variety of image features, describing the morphology of nerve fibres delineated either manually or automatically [13, 19, 20, 22, 23]. These studies have shown the relationship between several features, including those listed above, and neuropathic status. None of them, however, has addressed the question of diagnosis of individual subjects.

Here we describe the development of fibre detection described in [21] into a tool for automatic measurement of nerve fibre morphology to act as a diagnostic aid. We have previously reported clinical results of applying this system to DSPN [24]. In this paper we describe the algorithmic details and technical validation. We compare the fibre detector with another, successful, linear feature descriptor and demonstrate the best reported performance in detecting nerve fibres. We present algorithms for quantification of morphometric features, including the established features (CNFD, CNFL, CNBD) and novel features: Corneal Nerve Fibre Width Histogram (CNFWH) and Corneal Nerve Fibre Orientation Histogram (CNFOH).

Finally, we report a technical validation ofthe proposed system based on CCM images obtained from 84 control subjects and 92 type 1 diabetic patients.

2 METHODS

2.1 CCM Images and Manual Measurement

CCM images (Fig. 1a) were captured from all participants using the Heidelberg Retina Tomograph Rostock Cornea Module (HRT-III) as described in[13]. The image dimensions are 384×384 pixels with the pixel size of 1.0417µm. During CCM scan, images captured from all corneal layers and six sub-basal images from the right and left eyes were selected for analysis. Criteria for image selection were depth, focus position and contrast. A single experienced examiner, masked from the outcome of the medical and peripheral neuropathy assessment, manually quantified images of all study participants using purpose-writtenproprietary software (CCMetrics: M. A. Dabbah, Imaging Science, University of Manchester) to delineate main fibres, branch fibres and branch points (red lines, blue lines and green dots respectively in Fig. 1b). The reproducibility and reliability of manual annotation are reported in [15]. The specific parameters measured in each frame were: Corneal Nerve Fibre Density (CNFD), Corneal Nerve Fibre Length (CNFL) and Corneal Nerve Branch Density (CNBD), as described in section 1 in accordance with our previously published protocol [13].

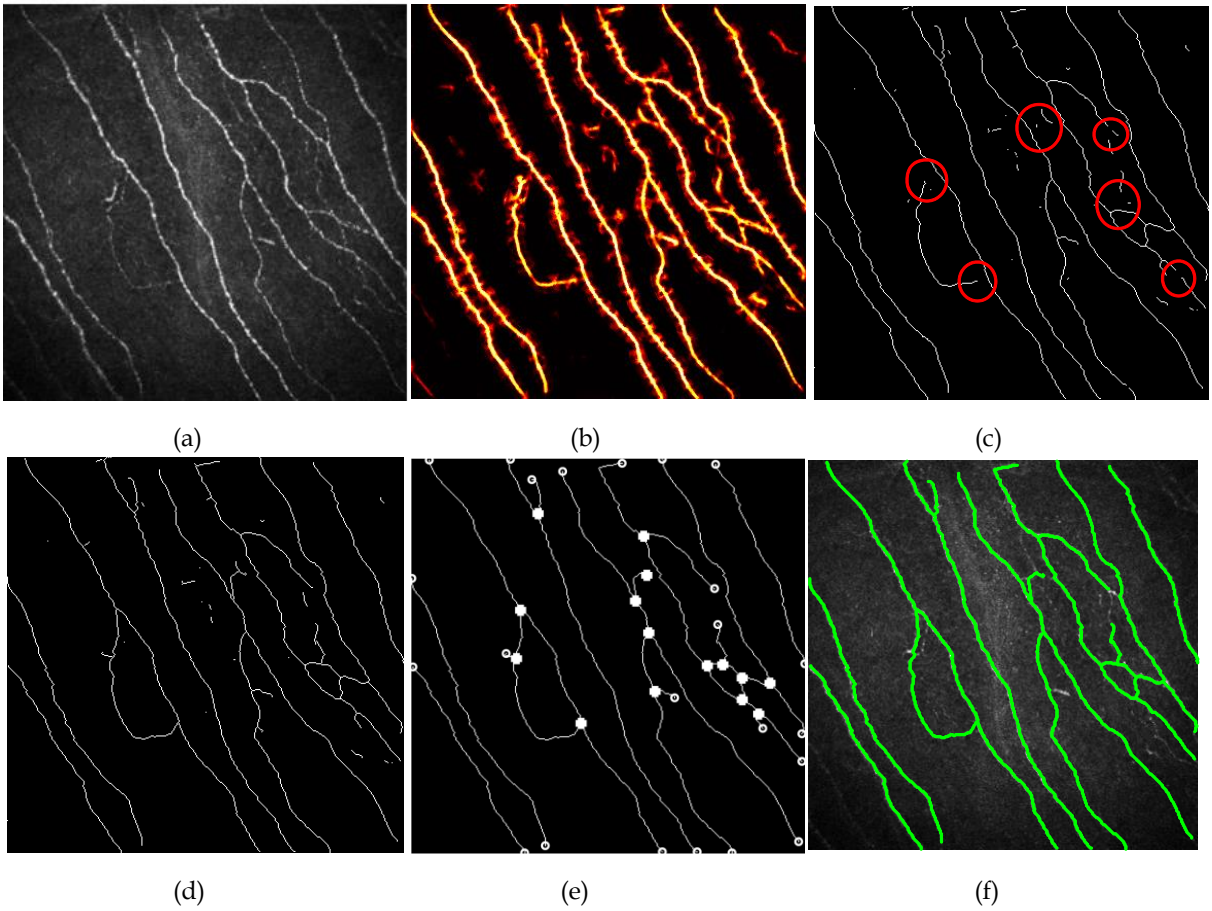

Fig. 2. (a) Original CCM image (b) Response image after nerve fibre detection (c) Nerve Fibre skeleton with highlighted weak connection segments (d) Nerve fibre skeleton after assessment of weak connections. (e) Automatically detected end points (hollow circles) and intersection points (solid circle). (f) Final detected nerve fibres.

2.2 Automated CCM Measurement

The automated CCM measurement process consists of two main steps: nerve fibre detection and nerve fibre quantification.

2.2.1 Nerve Fibre Detection

In this and similar applications [16, 17], methods based on machine learning have been reported to outperform others in detection of curvilinear features. The machine learning method normally consists of two key elements, feature description and classifier training on a set of samples.

For the feature description process, we have implemented and adapted two of the most successful methods [17, 21] for representing curvilinear structures. Dabbah et al. [23] proposed a "dual-model filter" (DMF) that combines a foreground model based on a Gabor wavelet with a Gaussian background model that scales the output according to the level of noise. In [21] a multi-scale version of this detector was described, applying the DMF ateight orientations and at four levels of an image pyramid to produce a multi-dimensional feature descriptor for each training pixel. Berks et al. [17], seeking to enhance linear structures in mammograms, used the dual-tree complex wavelet transform (DTW) [25] to represent the characteristic at each training pixel location also in a multi-resolution manner. The DTW produces a response at each pixel that consists of a 2 (magnitude and phase information) ×O ×N dimensional vector. O and N are the number of filter orientations and the number of the levels in the image pyramid respectively.

Both of these detectors outperformmed competitors in their respective domains. In this study we have subjected them to a comparative analysis in detecting nerve fibres. For classifier training, the feature descriptors and their corresponding fibre/non-fibre labels from a set of training samples were used as the inputs to a classifier, which took the form ofeither a neural network orrandom forest [22]. The trained classification model was then used for classifying fibre/non-fibre pixels in unseen CCM images. Fig. 2b shows the output response image resulting from the DMF and trained neural net classifier for an unseen CCM image (Fig. 2a). The evaluation and comparison of different combinations of the two feature descriptors and the two classifiers are presented in section 3.

A threshold is applied to the response image to generate a binary image. The optimum threshold value is determined by the Receiver Operating Characteristic (ROC) curve described in section 3.1. The binary image is then filtered by morphological operators to fill small gaps within nerve fibres and link adjacent structures. The binary structures are thinned to obtain the one-pixel wide skeleton (Fig. 2c). Branch and end points, identified by counting the neighbours of each skeleton point, are each assigned a unique label. For some regions, the evidence for nerve fibres is too weak (as highlighted in Fig. 2c) to

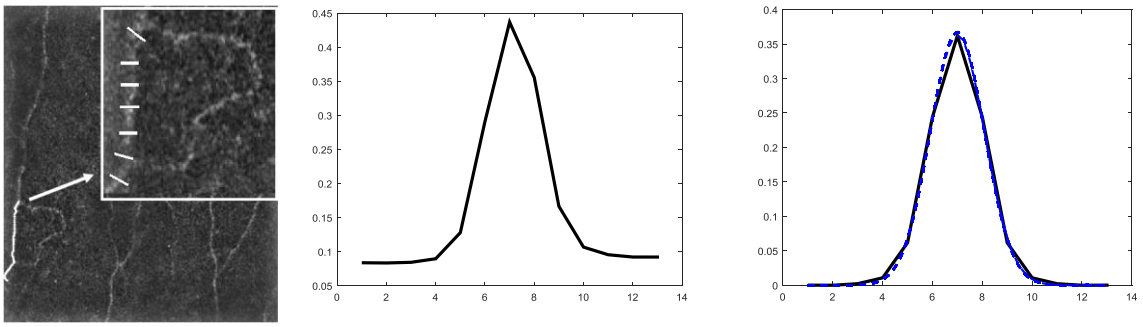

(a) (b) (c)

Fig. 3. (a) Original CCM image with a highlighted segment, a selection of orthogonal profile lines are indicated on the enlarged inset. Profiles are calculated at each pixel along the segment. (b) Average of all the profile lines along the whole fibre segment. (c)The symmetric profile of (b) is firstly calculated, and then normalised (Solid line). A Gaussian distribution is fitted for nerve fibre width estimation (dash line). The final width equals 2.5 times the RMS width (σ) of the fitted Gaussian curve.

be detected by a global threshold. However, the undetected pixels may be important in determining the nerve-fibre connectivity. Hence, for each end point, we extrude 30 pixels along the fibre orientations. The orientation of nerve fibres at each pixel location can be estimated using the second eigenvalue of the Hessian matrix of the response image. If an intersection with another fibre is detected and the average probability from the response image of the extruded pixels is sufficiently high (> 0.2), the extruded line is retained, otherwise it is eliminated (Fig. 2d). Subsequently, independent small segments and short branches that are less than 15 pixels long are removed, and the intersection points (solid circles) and end points (hollow circles) are calculated again as shown in Fig. 2e. The final binary skeleton, as shown in Fig. 2f, is used for total nerve fibre quantification, described in the next section.

2.2.2 Nerve Fibre Quantification

Fig. 2f shows that the output of fibre detection consists of several networks of interconnected line segments. In order to produce similar results to the manual CNFD, CNFL and CNBD, it is important to identify the main fibres within these networks and the branch points along the main fibres. To connect the appropriate fibre segments together, we generate four N × N matrices (MI, ML, MW and MO) to store the fibre intensity, fibre length, fibre width (described later in this section) and fibre orientation information respectively for each segment. N is the total number of branch and end points. If the i^{th} and j^{th} end/branch points are connected by a segment, the intensity, width, length and orientation information will be saved at the [i, j] location of the corresponding matrices; if they are not connected, these elements are zero. The matrices of intensity (MI), length (ML) and width (MW) are symmetric, as the elements at [i, j] and [j, i] should be identical. The [i, j] and [j, i] elements in the orientation matrix MO represent the respectiveorientations of the oppositeends of the fibre segment.

Identification of the main nerve fibres starts with the most prominent segments: those with greatest length and width. These are identified by multiplying the corresponding elements of MW and ML to produce a new matrix MA. The segments are considered in sequence according to the corresponding values of MA in descending order. There are normally two candidate segments that intersect with the current segment at a branch point. The candidate segments are ranked for the length, orientation difference, intensity and width parameters respectively. The candidate with the highest summed rank is chosen to connect with the current segment. The process continues till an end point is reached. The relevant entry in MA is set to zero and the process continues until no non-zero elements remain in MA. Finally, a list of connected fibres is obtained. Only the fibres with length greater than a threshold are kept as the main fibres. Fig. 1b and 1c respectively show the manual and automatic quantification results of the CCM image in Fig. 1a. The red lines show the principal nerve fibres, which are counted to produce CNFD. The blue lines indicate the secondary nerve fibres, which together with the principal fibres make up CNFL. The green dots are the branch points from the main fibres that are used for CNBD calculation.

Besides the CNFD, CNFL and CNBD features that are readily measured in the manual analysis, automatic quantification is able to calculate additional features. These additional CCM features include the total corneal nerve fibre area per mm^2 (CNFA), the corneal nerve fibre width histogram (CNFWH) and the corneal nerve fibre orientation histogram (CNFOH). These can be calculated if the width and orientation at each nerve fibre location is known. The orientation is calculated by the Hessian method referred toin section 2.2.1. The nerve fibre width estimation for a particular segment is illustrated in Fig. 3. Fig. 3a shows a highlighted example nerve fibre segment along with a magnified version. At each nerve fibre location, an intensity profile line of length 13 pixels (larger than the thickest fibre) is extracted perpendicular to the nerve fibre orientation, as indicated by the short straight lines in Fig. 3a. The profiles corresponding to a fibre segment are averaged along the length of the segment to generate a representativeprofile for the segment, which is then further averaged (Fig. 3b) with its symmetrically inverted profile, smoothed by a three pixel length average filter and normalised (Fig. 3c). Finally a Gaussian distribution is fitted to the normalised profile curve (Fig. 3c). The final width of that segment is calculated as 2.5 (empirically determined) times the RMS widthof the fitted

Gaussian curve. CNFWH is the number of occurrences of different fibre widths in the range between 1 to 8 pixels, at 0.2 pixels interval (36 bins).The CNFA is calculated as sum of fibre width × fibre length of all the fibre segments in mm^2. The CNFOH is the number of occurrences of different fibre orientations in the range between 0° to 179°, at 5 degree interval (36 bins).

3 Materials and Evaluation

The evaluation was conducted on a database that contained 888 images captured from 176 subjects (84 controls and 92 diabetic patients). The subjects were divided into 3 groups: control (n=84), type 1 diabetic patient with noneuropathy (n=63) and diabetic patients with neuropathy (n=29). The Toronto Diabetic Neuropathy Expert Group (TC) [6] recommendation was followed to define an individual to have DSPN if he/she met both of the following criteria: (1) Abnormal nerve conduction – A peroneal motor nerve conduction velocity of <42 m/s; (2) a symptom or sign of neuropathy, defined as ONE of the following: (a) diabetic neuropathy symptom (DNS)[28]of 1 or more out of 4, (b) neuropathy disability score (NDS)[28]of 3 or more out of 10. These features, along with a number of other clinical and physiological parameters, were measured for each subject [24].

3.1 Evaluation of Nerve Fibre Detection

For the nerve fibre detection evaluation, we randomly chose 50 images for training, and the remaining 838 images for testing. In the case of the dual-model feature descriptor, we followed [21] in using 32 dimensional vectors (8 orientations x 4 scale pyramid levels) to describe features at each pixel location. The dual-tree complex wavelet feature descriptor was a 6 (orientations) x 2 (real and imaginary parts of DWT) x 4 (image pyramid) dimensional vector at each pixel location. The two feature descriptors were then classified as fibre or background pixels using both Random Forest (RFC) and multi-layer perceptron neural network classifiers (NNC). We optimised performance by varying the number of training pixels (500, 1000, 2000 pixels randomly selected from each of foreground and background regions for each image), the number of trees (100, 200 and 500 trees) in RFC and the number of hidden neurons (20, 50 and 100) in the three-layer NNC. The response images were thresholded andthen thinned to one-pixel wide lines. These lines were then compared pixel by pixel to the manually generated skeletons acting as ground-truth, a true positive being scored if the detected pixel is within a three-pixel tolerance of ground truth and a false positive if it is outside this tolerance. By varying the threshold of the response images, ROC curves can be generated for each of the parameter settings. Optimum performance, in terms of detection accuracy and computation time, was achieved by using 2000 foreground and background pixels from each image for training, and 200 trees for RFC and 50 hidden neurons for NNC.

In Fig. 4, we only show the ROC curves based on the optimum parameter settings for the four combinations of feature descriptors and classifiers: DMF + RFC (DMRF), DMF + NNC (DMNN), DTW + RFC (DTRF) and DTW + NNC (DTNN). From the ROC curves, it is clear that the combination based on the DMF outperforms the DTW feature descriptor. Using the NNC classifier performed slightly, though not significantly, better than RFC in our dataset, using either feature detector. We achieved a better detection results than reported in [21] as our training was based on 50 randomly selected images whereas [21] was based on a single CCM image. We also tested the reliability of the training and prediction process. The process was repeated 10 times using the DMNN method with a different set of 50 randomly selected independent training images, using the remaining images for testing. The average sensitivity and specificity at equal error rate were 95.53% ±0.31% and 94.93% ±0.26% respectively, showing the high repeatability and reliability resulting from the use of the current parameter settings.

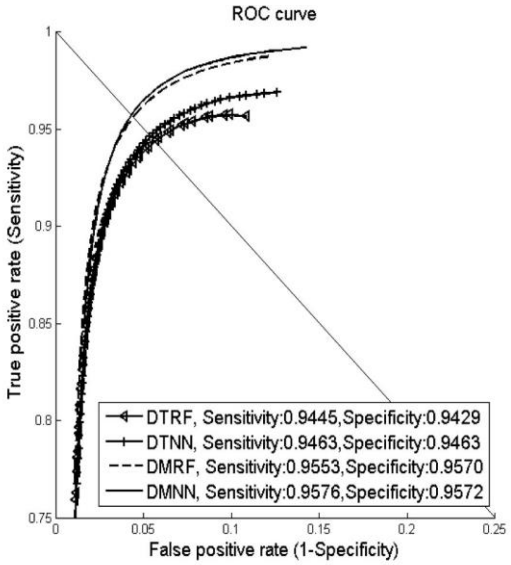

Fig. 4. ROC curves for nerve fibre detection using DMRF (Dual Model, Random Forest), DMNN (Dual Model, Neural Network), DTRF (Dual-Tree Wavelet, Random Forest) and DTNN (Dual-Tree Wavelet, neural Network) respectively.

3.2 Evaluation of Nerve Fibre Quantification

Corneal nerve-fibre density, corneal nerve fibre length and corneal nerve branch density (CNFD, CNFL and CNBD) were measured manually in each of the images using the CCMetrics annotation tool (denoted MCNFD, MCNFL, and MCNBD, respectively).

Corresponding automated measurements, denoted ACNFD, ACNFL and ACNBD, were calculated using the proposed system in addition to total nerve-fibre area, orientation histogram and width histogram (CNFA, CNFOH and CNFWH).For the multi-dimensional features CNFOH and CNFWH, we investigated the use of the maximum, standard deviation, skewness, kurtosis and logistic regression of combing all elements of the histogramfeature vectors to represent the feature. The stand-

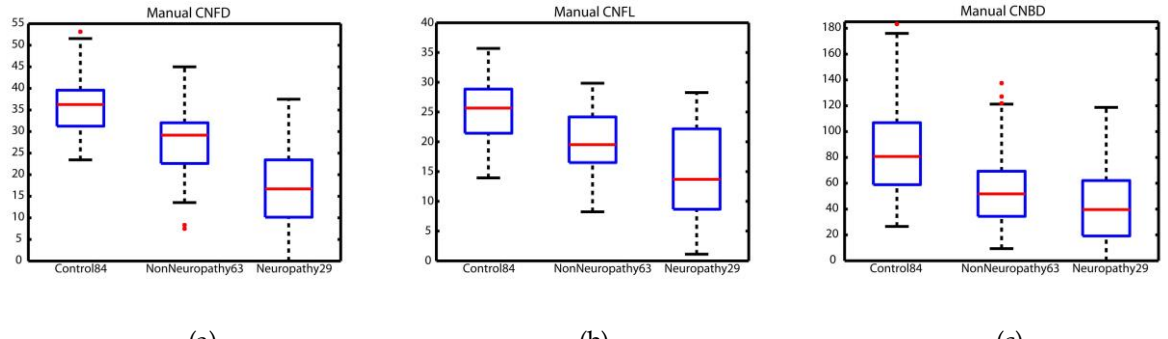

Fig. 5. Boxplots of manually measured features for control, non-neuropathy and neuropathy groups (a) MCNFD (b) MCNFL (c) MCNBD.

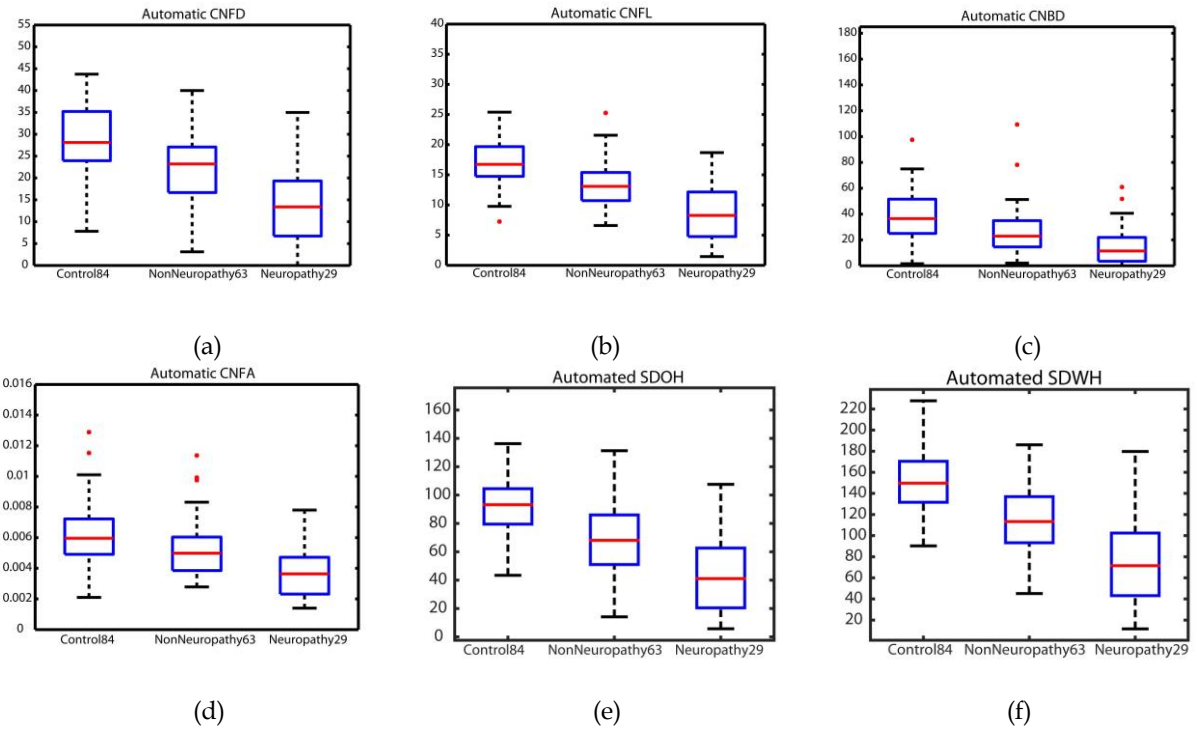

Fig. 6. Boxplots of automatically measured features for control, non-neuropathy and neuropathy groups (a) ACNFD (b) ACNFL (c) ACNBD (d) CNFA (e) SDOH (f) SDWH.

ard deviation of the histogram proved to be the most effective; these are denoted as SDOH and SDWH.

For each of the subjects, the average feature values obtained from their CCM images were used. Fig. 5 and Fig. 6 show the box plots of each of the manual and automated CCM features respectively. In Fig. 5 and Fig. 6, the central red lines are the median, the edges of the box are the 25th and 75th percentiles (q1 and q3), and the whiskers extend to the most extreme data points that are not identified as being outliers (within the range q1-1.5(q3-q1) to q3+1.5(q3-q1). The outliers are plotted individually as red dots. A common decreasing trend from control group to neuropathy group can be observed on all manual and automated CCM features. The Pearson correlation coefficients between automatically and manually derived CNFL, CNFD and CNBD measurements were 0.878, 0.870 and 0.723 respectively. The relatively lower correlation between manual and automatic CNBD measurement is due to poor reproducibility in the manual measurement of this feature. This has been reported in [15] and arises from the subjective judgement required for identifying branch points.

We used both the ANOVAtest [29] and ROC analysis to demonstrate the capability of using the CCM image features to discriminate between control and non-neuropathic groups, and between non-neuropathic and neuropathic patients, as defined by the Toronto Criteria.

Tables 1 and 2 show the respective ANOVA p-values, the area under the ROC curve (AUC) measures and sensitivity and specificity values calculated at the equal error point (EEP) of the ROC curves. We experimented with different combinations of features, from both manual and automated analysis, using logistic regression in a leave-one-out manner. In these experiments each subject was predicted by the logistic regression model built from the remaining n-1 subjects, where n is the total number of subjects in both groups. None of the combined features performed better than the best single features. For comparison, ROC measures for the combinations of all manual features or all automated features are listed in Table 1

TABLE 1
AUC, 95% CONFIDENCE INTERVAL VALUES AND SENSITIVITY-SPECIFICITY AT THE EQUAL-ERROR POINT (EEP) FOR MANUAL AND AUTOMATED CCM FEATURES FOR DISCRIMINATION BETWEEN **CONTROL SUBJECTS** AND **DIABETIC PATIENTS** WITHOUT DSPN.

CCM Features	AUC	95% CI	Sensitivity Specificity at EEP	p-value of ANOVA
MCNFD	**0.8063**	**[0.73 0.88]**	**0.7460**	**<0.0001**
MCNFL	0.7627	[0.68 0.84]	0.6825	<0.0001
MCNBD	0.7492	[0.67 0.83]	0.6984	<0.0001
ACNFD	0.7442	[0.66 0.82]	0.7302	<0.0001
ACNFL	**0.7814**	**[0.70 0.86]**	**0.7778**	**<0.0001**
ACNBD	0.7303	[0.65 0.81]	0.6667	<0.0001
CNFA	0.6802	[0.59 0.77]	0.6508	0.0002
SDOH	0.7663	[0.69 0.85]	0.6984	<0.0001
SDWH	0.7884	[0.71 0.86]	0.7302	<0.0001
Combined manual	0.7940	[0.72 0.87]	0.7143	-
Combined automated	0.7477	[0.67 0.83]	0.7143	-

TABLE 2
AUC, 95% CONFIDENCE INTERVAL VALUES AND SENSITIVITY-SPECIFICITY AT THE EQUAL-ERROR POINT (EEP) FOR MANUAL AND AUTOMATED CCM FEATURES FOR DISCRIMINATION BETWEEN **NON-NEUROPATHIC** AND **NEUROPATHIC** GROUPS OF DIABETIC PATIENTS.

CCM Features	AUC	95% CI	Sensitivity Specificity at EEP	p-value of ANOVA
MCNFD	**0.7890**	**[0.68 0.90]**	**0.7241**	**<0.0001**
MCNFL	0.7137	[0.59 0.83]	0.6552	0.001
MCNBD	0.6136	[0.49 0.74]	0.5862	0.081
ACNFD	0.7729	[0.66 0.88]	0.6552	<0.0001
ACNFL	0.7646	[0.65 0.88]	0.6207	<0.0001
ACNBD	0.7001	[0.58 0.82]	0.5862	0.002
CNFA	0.7542	[0.64 0.87]	0.7241	<0.0001
SDOH	0.7871	[0.68 0.90]	0.6897	<0.0001
SDWH	**0.7772**	**[0.67 0.88]**	**0.7241**	**<0.0001**
Combined manual	0.7843	[0.68 0.89]	0.7100	-
Combined automated	0.7531	[0.64 0.87]	0.6897	-

and Table 2 along with the single-feature measures.

4 Discussions and Conclusion

A number of studies have shown the features extracted from Corneal Confocal Microscopy images are associated with the severity of diabetic peripheral neuropathy [7, 12, 13] and the potential of CCM to quantify severity of neuropathy and assess therapeutic benefit has been demonstrated [19]. In this paper, we have presented the details of a complete system that is able to automatically quantify six different types of nerve fibre features in CCM images. We have proposed an optimum configuration for detection of nerve fibres based on a previously reported foreground and background model trained with a neural network. The automatic quantification results show a high correlation with manually measured CCM features (CNFL, CNFD and CNBD). The automated system is also able to produce additional CCM features that measure the area, width and orientation of the nerve fibres (CNFA, CNFWH and CNFOH). All these measures show significant differences between the non-neuropathic and neuropathic groups (p-values of ANOVA test in table 2), with some features achieving 72% sensitivity/specificity at the equal error rate point, indicating the capacity to identify individuals suffering from neuropathy. Our results also show significant differences (p-values of ANOVA test in table 1) between the control and non-neuropathic group, indicating the system's ability to detect early signs of change from a healthy to a diabetic condition.

Petropoulos et al. [24]reported a clinical evaluationstudy comparing the system described in this paper with manual analysis of CCM images and a broader range of subjective and objective clinical assessment methods, including the Neuropathy Symptom Profile, vibration perception thresholds, cool and warm thermal thresholds, and cold and heat induced pain. Electrophysiology tests included, in addition to PMNCV, peroneal motor nerve amplitude, sural sensory nerve amplitude and sural sensory nerve conduction velocity.CCM features, measured both automatically and manually, were found to be significantly correlated with these methods.They noted that the automatic analysis of CCM images was significantly faster than manual analysis, taking 10-22s per image, depending on the density of fibres, as opposed to 2-7 minutes.

Based on the well-established Toronto Criteria, we show that both manual and automated CCM features discriminate diabetic patients with and without neuropathy. Manual and automatic measurement regimes result in broadly similar results: about 0.78 AUC value and 72% sensitivity-specificity at the equal error rate point. There were no significant differences between the ROCs of manual (MCNFD) and automated measurements (e.g. p=0.42 and 0.57 for ACNFD and SDWH respectively). The advantages in time labour and reproducibility sug-

gest that automatically measured features may be used as a new, non-invasive method for diagnosing diabetic peripheral neuropathy, providing information on small nerve fibre damage that is not accessible by most currently used methods. The only method which addresses small fibre damage is the intra-epidermal nerve fibre density (IENFD) measure, which is invasive, requiring a skin biopsy and currently cannot be evaluated automatically. We have recently shown [30] that analysis of CCM features has comparable diagnostic efficacy to IENFD.

Corneal confocal microscopy has shown considerable success in translation to the assessment of other neuropathies including Fabry disease [31], ISFN [32], CMT1A [33], sarcoidosis [34]. Automated quantification of corneal nerves provides a major step forward in the early diagnosis and assessment of progression, but in particular for use in clinical trials to establish therapeutic benefit in diabetic and other peripheral neuropathies.

The automatic quantification software can be requested freely from [35] for research purposes. It is currently being used by over 40 research groups worldwide to investigate potential relationships between CCM features and different types of neuropathy [36].

ACKNOWLEDGMENT

Thisresearch was funded by awards from: National Institutes of Health (R105991) and Juvenile Diabetes Research Foundation International (27-2008-362).

REFERENCES

[1] A. J. Boulton, “Management of Diabetic Peripheral Neuropathy,” *Clinical Diabetes,* vol. 23, no. 1, pp. 9-15, 2005.

[2] C. Daousi, I. A. MacFarlane, A. Woodward, T. J. Nurmikko, P. E. Bundred, and S. J. Benbow, “Chronic painful peripheral neuropathy in an urban community: a controlled comparison of people with and without diabetes,” *Diabetic Medicine,* vol. 21, no. 9, pp. 976-982, Sep, 2004.

[3] P. J. Dyck, C. J. Overland, P. A. Low, W. J. Litchy, J. L. Davies, P. C. O’Brien, C. v. N. T. Investigators, J. W. Albers, H. Andersen, C. F. Bolton, J. D. England, C. J. Klein, J. G. Llewelyn, M. L. Mauermann, J. W. Russell, W. Singer, A. G. Smith, S. Tesfaye, and A. Vella, “Signs and symptoms versus nerve conduction studies to diagnose diabetic sensorimotor polyneuropathy: CI vs. NPhys trial,” *Muscle Nerve,* vol. 42, no. 2, pp. 157-164, 2010.

[4] P. J. Dyck, J. W. Albers, J. Wolfe, C. F. Bolton, N. Walsh, C. J. Klein, A. J. Zafft, J. W. Russell, K. Thomas, J. L. Davies, R. E. Carter, L. J. Melton, W. J. Litchy, and C. v. N. T. Investigators, “A trial of proficiency of nerve conduction: greater standardization still needed,” *Muscle nerve,* vol. 48, no. 3, pp. 369-374, 2013.

[5] P. J. Dyck, J. E. Norell, H. Tritschler, K. Schuette, R. Samigullin, D. Ziegler, E. J. Bastyr, W. J. Litchy, and P. C. O’Brien, “Challenges in Design of Multicenter Trials: Endpoints Assessed Longitudinally for Change and Monotonicity,” *Diabetes Care,* vol. 30, pp. 2619-2625, 2007.

[6] S. Tesfaye, A. J. Boulton, P. J. Dyck, R. Freeman, M. Horowitz, P. Kempler, G. Lauria, R. A. Malik, V. Spallone, A. Vinik, L. Bernardi, and P. Valensi, “on behalf of the Toronto Diabetic Neuropathy Expert Group, Diabetic neuropathies: Update on definitions, diagnostic criteria, estimation of severity, and treatments,” *Diabetes Care,* vol. 33, no. 10, pp. 2285-2293, 2010.

[7] P. Hossain, A. Sachdev, and R. A. Malik, “Early detection of diabetic peripheral neuropathy with corneal confocal microscopy,” *The Lancet,* vol. 366, no. 94, pp. 1340-1343, 2005.

[8] N. Pritchard, K. Edwards, A. W. Russell, B. A. Perkins, R. A. Malik, and N. Efron, “Corneal confocal microscopy predicts 4-year incident peripheral neuropathy in type 1 diabetes,” *Diabetes Care,* vol. EPub ahead of print, 2015.

[9] M. Brines, A. N. Dunne, M. V. Velzen, P. L. Proto, C. G. Ostenson, R. I. Kirk, I. Petropoulos, S. Javed, R. A. Malik, A. Cerami, and A. Dahan, “ARA 290, a non-erythropoietic peptide engineered from erythropoiethin, improves metabolic control and neuropathic symptoms in patients with type 2 diabetes,” *Molecular Medicine,* vol. 6, 2014.

[10] M. Tavakoli, M. Mitu-Pretorian, I. N. Petropoulos, H. Fadavi, O. Asghar, U. Alam, G. Ponirakis, M. Jeziorska, A. Marshall, N. Efron, A. J. Boulton, T. Augustine, and R. A. Malik, “Corneal confocal microscopy detects early nerve regeneration in diabetic neuropathy after simultaneous pancreas and kidney transplantation,” *Diabetes Care,* vol. 62, no. 1, pp. 254-260, 2013.

[11] S. Azmi, M. Ferdousi, I. N. Petropoulos, G. Ponirakis, H. Fadavi, M. Tavakoli, U. Alam, and W. Jones, “Corneal confocal microscopy shows an improvement in small-fiber neuropathy in subjects with type 1 diabetes on continuous subcutaneous insulin infusion compared with multiple daily injection,” *Diabetes Care,* vol. 38, no. 1, pp. e3-e4, 2015.

[12] M. Tavakoli, C. Quattrini, C. Abbott, P. Kallinikos, A. Marshall, J. Finnigan, P. Morgan, N. Efron, A. Boulton, and R. Malik, “Corneal Confocal Microscopy: A Novel Non-invasive Test to Diagnose and Stratify the Severity of Human Diabetic Neuropathy,” *Diabetes Care,* vol. 33, no. 8, pp. 1792-1797, 2010.

[13] R. A. Malik, P. Kallinikos, C. A. Abbott, C. H. M. v. Schie, P. Morgan, N. Efron, and A. J. M. Boulton, “Corneal confocal microscopy: a noninvasive surrogate of nerve fibre damage and repair in diabetic patients,” *Diabetologia,* vol. 46, no. 5, pp. 683-688, 2003.

[14] C. Dehghani, N. Pritchard, K. Edwards, D. Vagenas, A. W. Russell, R. A. Malik, and N. Efron, “Morphometric stability of the corneal subbasal nerve plexus in healthy individuals: 1 3-year longitudinal study using corneal confocal microscopy,” *Invest Ophthalmol Vis. Sci.,* vol. 55, no. 5, pp. 3195-3199, 2014.

[15] I. Petropoulos, T. Manzoor, P. Morgan, H. Fadavi, O. Asghar, U. Alam, G. Ponirakis, M. Dabbah, X. Chen, J. Graham, M. Tavakoli, and R. Malik, “Repeatability of In Vivo Corneal Confocal Microscopy to Quantify Corneal Nerve Morphology,” *Cornea,* vol. 32, no. 5, pp. 83-89, 2013.

[16] M. Niemeijer, J. J. Staal, B. v. Ginneken, M. Loog, and M. D. Abramoff, “Comparative study of retinal vessel segmentation methods on a new publicly available database,” *SPIE Medical Imaging,* vol. 5370, pp. 648-656, 2004.

[17] M. Berks, Z. Chen, S. Astley, and C. Taylor, “Detecting and classifying linear structures in mammograms using random forests,” *IPMI 11 proceedings of the 22nd international conference on information processing in medical imaging*, pp. 510-524, 2011.

[18] F. Scarpa, E. Grisan, and A. Ruggeri, “Automatic Recognition of Corneal Nerve Structures in Images from Confocal Microscopy,” *Investigative Ophthalmology and Visual Science,* vol. 49, no. 11,

pp. 4801-4807, 2008.

[19] T. Holmes, M. Pellegrini, C. Miller, T. Epplin-Zapf, S. Larkin, S. Luccarelli, and G. Staurenghi, “Automated Software Analysis of Corneal Micrographs for Peripheral Neuropathy,” *Investigative Ophthalmology and Visual Science,* vol. 51, no. 9, pp. 4480-4491, 2010.

[20] C. W. Sindt, B. Lay, H. Bouchard, and J. R. Kern, “Rapid Image Evaluation System for Corneal In Vivo Confocal Microscopy,” *Cornea,* vol. 32, no. 4, pp. 460-465, 2013.

[21] M. A. Dabbah, J. Graham, I. N. Petropoulos, M. Tavakoli, and R. A. Malik, “Automatic analysis of diabetic peripheral neuropathy using multi-scale quantitative morphology of nerve fibres in corneal confocal microscopy imaging,” *Medical Image Analysis,* vol. 15, pp. 738-747, 2011.

[22] F. Scarpa, X. Zheng, Y. Obashi, and A. Ruggeri, “Automatic Evaluation of Corneal Nerve Tortuosity in Images from In Vivo Confocal Microscopy,” *Investigative Ophthalmology and Visual Science,* vol. 52, no. 9, pp. 6404-6408, 2011.

[23] M. A. Dabbah, J. Graham, M. Tavakoli, I. Petropoulos, and R. A. Malik, “Dual model automatic detection of nerve-fibres in corneal confocal microscopy images,” *MICCAI* vol. 6361, pp. 300-307, 2010.

[24] I. N. Petropoulos, U. Alam, H. Fadavi, A. Marshal, O. Asghar, M. A. Dabbah, X. Chen, J. Graham, G. Ponikaris, A. J. M. Boulton, M. Tavakoli, and R. A. Malik, “Rapid automated diagnosis of diabetic peripheral neuropathy with in vivo corneal confocal microscopy,” *Investigative Optics and Visual Science,* vol. 55, pp. 2071-2078, 2014.

[25] N. G. Kingsbury, “Complex wavelets for shift invariant analysis and filtering of signals,” *Journal of Applied and Computational Harmonic Analysis* vol. 10, no. 3, pp. 234-253, 2001.

[26] S. B. Kotsiantis, I. D. Zaharakis, and P. E. Pintelas, “Machine learning: a review of classification and combining techniques,” *Artificial Intelligence Review,* vol. 26, no. 3, pp. 159-190, 2006.

[27] J. W. G. Meijer, A. J. Smit, E. V. Sonderen, J. W. Groothoff, W. H. Eisma, and T. P. Links, “Symptom scoring systems to diagnose distal polyneuropathy in diabetes: the Diabetic Neuropathy Symptom score,” *Diabetic Medicine,* vol. 19, no. 11, pp. 962-965, 2002.

[28] M. J. Young, A. J. M. Boulton, A. F. Macleod, D. R. R. Williams, and P. H. Sonksen, “A multicentre study of the prevalence of diabetic peripheral neuropathy in the United Kingdom hospital clinic population,” *Diabetologia* vol. 36, pp. 150-154, 1993.

[29] K. Wallis, “Use of ranks in on-criterion variance analysis,” *Journal of the American Statistical Association,* vol. 47, no. 260, pp. 583-621, 1952.

[30] X. Chen, J. Graham, M. Dabbah, I. Petropoulos, G. Ponirakis, O. Asghar, U. Alam, A. Marshall, H. Fadavi, M. Ferdousi, S. Azmi, M. Tavakoli, N. Efron, M. Jeziorska and R. Malik, “Small nerve fiber quantification in the diagnosis of diabetic sensorimotor polyneuropathy: comparing corneal confocal microscopy with intraepidermal nerve fiber density,” Diabetes Care*,* vol. 38, no. 6, pp. 1138-1144, 2015.

[31] M. Tavakoli, A. Marshall, L. Thompson, M. Kenny, S. Waldek, N. Efron, and R. A. Malik, “Corneal confocal microscopy: a novel noninvasive means to diagnose neuropathy in patients with Fabry disease,” *Muscle Nerve,* vol. 40, no. 6, pp. 976-84, Dec, 2009.

[32] M. Tavakoli, A. Marshall, R. Pitceathly, H. Fadavi, D. Gow, M. E. Roberts, N. Efron, A. J. Boulton, and R. A. Malik, “Corneal confocal microscopy: a novel means to detect nerve fibre damage in idiopathic small fibre neuropathy,” *Exp Neurol,* vol. 223, no. 1, pp. 245-50, May, 2010.

[33]M. Tavakoli, A. Marshall, S. Banka, I. N. Petropoulos, H. Fadavi, H. Kingston, and R. A. Malik, “Corneal confocal microscopy detects small-fiber neuropathy in Charcot-Marie-Tooth disease type 1A patients,” *Muscle Nerve,* vol. 46, no. 5, pp. 698-704, Nov, 2012.

[34] M. van Velzen, L. Heij, M. Niesters, A. Cerami, A. Dunne, A. Dahan, and M. Brines, “ARA 290 for treatment of small fiber neuropathy in sarcoidosis,” *Expert Opin Investig Drugs,* vol. 23, no. 4, pp. 541-50, Apr, 2014.

[35] Accmetrics. "http://www.medicine.manchester.ac.uk/ena/."

[36] ENAgroup. "http://www.human-development.manchester.ac.uk/ena/ACCMetricsuserinstructions/."